Age-associated differences in the human lung extracellular matrix

Koloko Ngassie, Maunick Lefin; De Vries, Maaike; Borghuis, Theo; Timens, Wim; Sin, Don D; Nickle, David; Joubert, Philippe; Horvatovich, Peter; Marko-Varga, György; Teske, Jacob J

Published in:
American Journal of Physiology - Lung Cellular and Molecular Physiology

DOI:
10.1152/ajplung.00334.2022

Publication date:
2023

AMERICAN JOURNAL OF PHYSIOLOGY
LUNG CELLULAR AND MOLECULAR PHYSIOLOGY

Am J Physiol Lung Cell Mol Physiol 324: L799–L814, 2023.
First published April 11, 2023; doi:10.1152/ajplung.00334.2022

RESEARCH ARTICLE

Age-associated differences in the human lung extracellular matrix

Maunick Lefin Koloko Ngassie,[1,2] Maaike De Vries,[2,3] Theo Borghuis,[1] Wim Timens,[1,2] Don D. Sin,[4] David Nickle,[5] Philippe Joubert,[6] Peter Horvatovich,[7] György Marko-Varga,[8] Jacob J. Teske,[9] Judith M. Vonk,[2,3] Reinoud Gosens,[2,10] Y. S. Prakash,[9] Janette K. Burgess,[1,2]* and Corry-Anke Brandsma[1,2]*

[1]*Department of Pathology and Medical Biology, University Medical Center Groningen, University of Groningen, Groningen, Netherlands;* [2]*Groningen Research Institute for Asthma and COPD, University Medical Center Groningen, University of Groningen, Groningen, Netherlands;* [3]*Department of Epidemiology, University Medical Center Groningen, University of Groningen, Groningen, Netherlands;* [4]*Centre for Heart Lung Innovation at St. Paul's Hospital, University of British Columbia, Vancouver, British Columbia, Canada;* [5]*Monoceros Bio, San Diego, California, United States;* [6]*Institut Universitaire de Cardiologie et de Pneumologie de Québec, Quebec City, Quebec, Canada;* [7]*Department of Analytical Biochemistry, Groningen Research Institute of Pharmacy, University of Groningen, Groningen, Netherlands;* [8]*Center of Excellence in Biological and Medical Mass Spectrometry, Biomedical Center, Lund University, Lund, Sweden;* [9]*Department of Anesthesiology and Perioperative Medicine, Mayo Clinic, Rochester, Minnesota, United States; and* [10]*Department of Molecular Pharmacology, University of Groningen, Groningen, Netherlands*

Abstract

Extracellular matrix (ECM) remodeling has been associated with chronic lung diseases. However, information about specific age-associated differences in lung ECM is currently limited. In this study, we aimed to identify and localize age-associated ECM differences in human lungs using comprehensive transcriptomic, proteomic, and immunohistochemical analyses. Our previously identified age-associated gene expression signature of the lung was re-analyzed limiting it to an aging signature based on 270 control patients (37–80 years) and focused on the Matrisome core geneset using geneset enrichment analysis. To validate the age-associated transcriptomic differences on protein level, we compared the age-associated ECM genes (false discovery rate, FDR < 0.05) with a profile of age-associated proteins identified from a lung tissue proteomics dataset from nine control patients (49–76 years) (FDR < 0.05). Extensive immunohistochemical analysis was used to localize and semi-quantify the age-associated ECM differences in lung tissues from 62 control patients (18–82 years). Comparative analysis of transcriptomic and proteomic data identified seven ECM proteins with higher expression with age at both gene and protein levels: COL1A1, COL6A1, COL6A2, COL14A1, FBLN2, LTBP4, and LUM. With immunohistochemistry, we demonstrated higher protein levels with age for COL6A2 in whole tissue, parenchyma, airway wall, and blood vessel, for COL14A1 and LUM in bronchial epithelium, and COL1A1 in lung parenchyma. Our study revealed that higher age is associated with lung ECM remodeling, with specific differences occurring in defined regions within the lung. These differences may affect lung structure and physiology with aging and as such may increase susceptibility to developing chronic lung diseases.

NEW & NOTEWORTHY We identified seven age-associated extracellular matrix (ECM) proteins, i.e., COL1A1, COL6A1, COL6A2 COL14A1, FBLN2, LTBP4, and LUM with higher transcript and protein levels in human lung tissue with age. Extensive immunohistochemical analysis revealed significant age-associated differences for COL6A2 in whole tissue, parenchyma, airway wall, and vessel, for COL14A1 and LUM in bronchial epithelium, and COL1A1 in parenchyma. Our findings lay a new foundation for the investigation of ECM differences in age-associated chronic lung diseases.

aging; airway wall; extracellular matrix; lung; parenchyma

INTRODUCTION

Aging is a natural phenomenon that affects molecular and biological processes and subsequently also the structure and function of tissues and organs including the lung, contributing to the impairment of the tissue and organ homeostasis (1). Lung aging is characterized by structural and physiological differences including the larger size of alveoli, less elasticity, thickening of the small airway wall, worse lung function, and remodeling of the extracellular matrix (ECM) (2–4). Significant changes such as decreased elastin and increased collagen deposition have been observed in lung

*J. K. Burgess and C.-A. Brandsma contributed equally to this work.
Correspondence: C.-A. Brandsma (c.a.brandsma@umcg.nl).
Submitted 5 October 2022 / Revised 15 February 2023 / Accepted 2 April 2023

ECM from old mice (5, 6). Several features of aging have been found to be more pronounced in chronic lung diseases including chronic obstructive pulmonary disease (COPD) with a high prevalence in the elderly (2, 7).

Given its role as a provider of the architectural structure, mechanical support, and regulator of several biological processes (8), the ECM plays an important role in organ homeostasis. The molecular composition, biological, and mechanical properties of the ECM are tissue specific (8). The lung ECM is composed of a complex combination of elastin, collagens, glycosaminoglycans, proteoglycans, and glycoproteins. Components of the ECM have specific functions in organs; accordingly, elastin provides the lung its extension and recoil properties (9), collagens provide tensile strength and regulate cellular migration and adhesion, glycosaminoglycans regulate growth factor activity and lung viscoelasticity through their hydration properties(8). In our previous study, a gene set enrichment analysis (GSEA) revealed a significant negative enrichment of the ECM-receptor interaction pathway with age in COPD compared with non-COPD tissue, indicating that ECM genes change differently with increasing age in COPD patients compared with controls (10). In addition, a recent publication highlighted the positive enrichment of genes of the ECM pathway with age in human lungs (11). Altogether, these studies suggest age-related alterations in lung ECM proteins; however, detailed knowledge is still scarce and information on regional differences within the lung is lacking.

In this study we examined the age-associated differences in ECM proteins at both transcriptional and protein levels in human lung tissue derived from patients with normal lung function and no history of chronic lung disease. In addition, we performed immunohistochemistry to assess age-associated ECM differences in specific lung compartments, i.e., whole lung tissue, lung parenchyma, airway wall, bronchial epithelium, and blood vessels.

MATERIALS AND METHODS

Ethics Statements

The study protocol was consistent with the Research Code of the University Medical Center Groningen [research code UMCG (umcgresearch.org)] and national ethical and professional guidelines [Code of conduct for Health Research (only in Dutch): Gedragscode-Gezondheidsonderzoek-2022.pdf (coreon.org)]. Lung tissues used in this study were derived from leftover lung material after lung surgery from archival materials that are exempt from consent in compliance with applicable laws and regulations [Dutch laws: Medical Treatment Agreement Act (WGBO) art 458/GDPR art 9/UAVG art 24]. This material was not subject to the Medical Research Human Subjects Act in the Netherlands, and, therefore, an ethics waiver was provided by the Medical Ethical Committee of the University Medical Center Groningen. All samples and clinical information were coded before experiments were performed, blinding all directly identifying information to the investigators.

Prior to the collection of lung tissue samples at St. Mary's Hospital, Mayo Clinic Rochester, MN, our study was approved by Mayo Clinic Institutional Review Boards. Patient informed consent (written or video/verbal) was obtained during clinic visits before surgical decisions. Upon acquisition of lung tissues, relevant clinical data were recorded, and the lung tissue samples were given unique numbers to provide anonymization.

Procurement of Lung Tissues

The transcriptomic (microarray) and proteomic data were derived from two previous studies described by De Vries et al. and Brandsma et al. (10, 12) and were obtained from lung tissues from control patients with normal lung function and no history of chronic lung disease. The lung tissues used for immunohistochemistry were derived from patients undergoing therapeutic lung resection surgery for cancer at the University Medical Center Groningen (Groningen, The Netherlands), which were part of the HOLLAND (HistopathOLogy of Lung Aging aNd COPD) project, or the Mayo Clinic (Rochester, MN). The HOLLAND project is a large immunohistochemistry study performed at the Department of Pathology and Medical Biology of the UMCG aiming to identify and correlate differences in several ECM, inflammatory, epithelial, and senescence markers in serial sections from the same lung in relation to chronic lung disease (i.e., COPD and IPF) and aging. All samples were obtained from non-involved peripheral lung tissue remaining after the diagnostic procedure as left-over material that can be used for medical research when no objection is made by the patient. Lung tissue samples used for transcriptomic, proteomic, and immunohistochemical analyses were collected in agreement with the ethical guidelines at the different collection sites (transcriptomic: Groningen, Vancouver, and Quebec, proteomic: Groningen) and were described in previous publications (13, 14). Macroscopically normal lung tissues were taken distant from the tumor. These tissues were fixed in formalin and embedded in paraffin. Then, histologically examined for abnormalities using standard hematoxylin and eosin (H&E) staining. The control patients from Groningen all had normal lung function, i.e., $FEV_1/FVC > 70\%$, no lung function data were available for the patients from Mayo Clinic. Patients were nonsmokers, ex-smokers, or current smokers, with an age range between 18 and 82 yr.

Transcriptomic Analyses

We re-analyzed our previously identified age-associated gene expression signature of the lung, limiting it to an aging signature based solely on the 270 nondisease control patients (10). In short, linear regression analysis adjusted for the potential confounders sex, smoking status (ex or current smokers), and technical variation using principal components explaining >1% of the variation was performed using R software. The three cohorts Groningen, Laval, and Quebec were analyzed separately and combined by a meta-analysis. To correct for multiple testing, the Benjamini–Hochberg false discovery rate (FDR) was applied. Next, we determined the enrichment of ECM-associated genes using Gene Set Enrichment Analysis (GSEA 4.1.0), including all genes present in the Matrisome geneset (NABA_Matrisome; M5889, Molecular Signatures Database v7.4). All Matrisome genes with a significant enrichment score were defined as our age-associated ECM genes.

Proteomic Analyses

We assessed the association between age and protein expression in nine nondisease control patients for which the data was derived from our previously published lung tissue proteomics data set (12). The edge R package version 4.1.0 was used for linear regression of the data following a negative binomial distribution and using edgeR. For this analysis

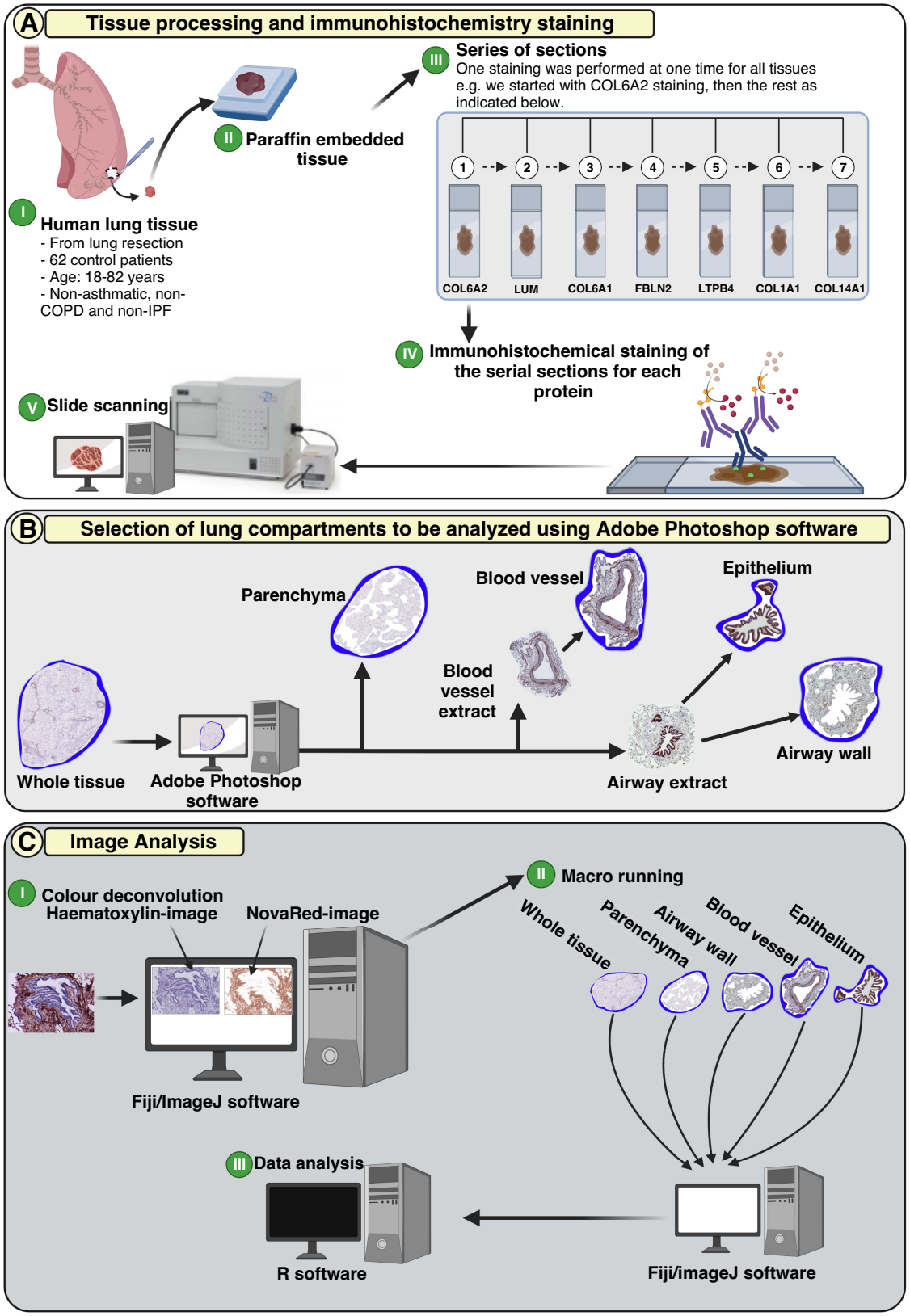

Table 1. *Patient characteristics transcriptomics cohort (10)*

	Groningen	Vancouver	Quebec
Number	45	90	135
Age, years, median (range)	60 (37–76)	62 (40–80)	62 (41–80)
Male/female, *N*	20/25	49/40	76/59
Smoking, *N*			
Ex	25	59	113
Current	20	31	22
Pack years, median (range)	35 (21–41)	37.75 (24–49.9)	38.35 (25–46)

only age was added as a factor in the regression analysis. FDR $P < 0.05$ was considered significant.

Immunohistochemical Staining

To localize the expression of the age-associated ECM proteins and to validate the transcriptomic and proteomic findings, immunohistochemical staining was performed in lung tissues derived from 62 control patients. The lung tissues were embedded in paraffin and cut into 6-μm thick sections. For the staining of the seven identified age-associated ECM proteins, for each protein, one section was analyzed per control patient. For each of the proteins, the sections from all subjects were stained in one batch at the same time to avoid batch effects. These sections were deparaffinized and rehydrated; followed by antigen retrieval with 10 mM citrate buffer pH6 for COL1A1, FBLN2, LTBP4, and LUM stainings and 10 mM Tris/EDTA buffer pH9 for COL6A1, COL6A2, and COL14A1 stainings. Endogenous peroxidase activity was blocked by 0.3% hydrogen peroxidase (H_2O_2), followed by overnight incubation at 4°C of the primary antibodies COL1A1 (monoclonal mouse, anti-human, ab88147, 1:400, abcam), COL6A1 (polyclonal rabbit, anti-human, NB120-6588, 1:3200, Novus Biologicals), COL6A2 (monoclonal rabbit, anti-human, ab180855, 1:12500, abcam), COL14A1 (polyclonal rabbit, anti-human, HPA023781, 1:100, Atlas Antibodies), FBLN2 (polyclonal rabbit, anti-human, HPA001934, 1:400, Atlas Antibodies), LTBP4 (polyclonal rabbit, anti-human, ab222844, 1:400, abcam), and LUM (monoclonal rabbit, anti-human, ab168348, 1:12500, abcam) diluted in a 1% BSA-PBS. The sections were washed and incubated with the Horseradish peroxidase (HRP)-conjugated secondary antibodies diluted (1:100) in 2% human serum + 1% BSA-PBS, i.e., polyclonal Goat Anti-Rabbit (P0488, Dako, Denmark) for COL6A1, COL6A2, COL14A1, FBLN2, LTBP4, and LUM and polyclonal Rabbit Anti-Mouse (P0260, Dako, Denmark) for COL1A1 staining. Negative controls (no primary antibody controls) were also included. Positive staining was visualized using 5-min incubation with Vector NovaRED Substrate (SK-4800, Vector Laboratories, Canada). Sections were counterstained with hematoxylin, mounted and scanned using the ×40 objective of the Hamamatsu NanoZoomer 2.0HT digital slide scanner (Hamamatsu Photonic K.K., Japan). The digital images were viewed with Aperio ImageScope V.12.4.3 (Leica Biosystems, Germany). Figure 1*A* summarizes the immunohistochemical staining process.

Image Analyses

Different compartments of the lung including whole lung tissue, parenchyma, airway wall, bronchial epithelium, and blood vessels were analyzed for the expression and distribution of stained ECM proteins. The extraction of the lung compartments was performed by one person in a blinded manner. First, images containing whole lung tissue, airways, and blood vessels were extracted from the scans using Aperio ImageScope software V.12.4.3 (Leica Biosystems, Nussloch, Germany). Depending on how many airways and blood vessels were present in the tissue, up to 10 airways or blood vessels were extracted. Next, Adobe Photoshop software (Adobe Inc. CA) was used to extract the specific area of interest for analysis (Fig. 1*B*), i.e., parenchyma excluding airway and vessels, airway wall from basement membrane to alveolar attachments, bronchial epithelial layer from basement membrane to ciliary layer and blood vessel walls from endothelium to alveolar attachment except for LUM (from tunica media to endothelium), since LUM was localized in that specific region. Artifacts including carbon pigments, folded tissue, red blood cells, and mucus plugs were removed. Fiji/ImageJ software (15) was used to quantify the intensity and area of positive staining (Fig. 1*C*). The whole tissue, parenchyma, airway wall, bronchial epithelium, and blood vessel were all analyzed separately. All image files were separated into blue (hematoxylin-image), and red (NovaRed-image) pixels using color deconvolution plugin by Landini et al. (16). To determine the correct optical density vectors for the red-green-blue (RGB) channel of hematoxylin and NovaRed, we followed the protocol as previously described by Ruifrok et al. (17). A vector was developed to receive automated numbers for each pixel in the different images. To calculate the total amount of tissue, images were converted to 8-bit grey scale. Total number of pixels representing total tissue area versus positively stained tissue area were identified using the threshold feature of Fiji/ImageJ

Figure 1. Tissue processing, immunohistochemistry, and image analysis. *A*: lung tissues were embedded in paraffin and cut in serial sections. The sections were then immunohistochemically stained for ECM proteins including, COL1A1, COL6A1, COL6A2, COL14A1, FBLN2, LTBP4, and LUM. After the staining, the images were captured using the Hamamatsu NanoZoomer 2.0HT digital slide scanner at magnification of ×40. *B*: the digital images were checked for their quality and once validated the whole tissue, parenchyma, airway wall, airway epithelium and blood vessel wall areas were isolated and cleaned (artifacts were removed). *C*: for the image analysis, a vector was developed to separate the hematoxylin and NovaRed image components using the color deconvolution plugin in ImageJ. Afterwards, a specific developed macro was run for each staining, followed by data analysis using R software. COL1A1, collagen type I α 1; COL6A1, collagen type VI α 1; COL6A2, collagen type VI α 2; COL14A1, collagen type XIV α 1; FBLN2, fibulin-2; LTBP4, latent transforming growth factor beta binding protein 4; LUM, lumican. [Image created with BioRender.com and published with permission.]

Table 2. *Patient characteristics proteomics cohort*

	Age, Years, Median (Range)	Male/Female, N	Packyears, N	FEV_1%Pred	FEV_1/FVC Ratio
Non-COPD control (N = 9)	67 (49–76)	4/5	34 (17)*	94 (10)	76 (4)

Mean (SD) was calculated for packyears, FEV_1% and FEV/FVC ration. *Two controls had missing info for packyears, FEV_1: forced expiratory volume in 1 s, FVC: forced vital capacity.

software. The percentage of positive area and the mean intensity were calculated using the following formulas, where the percentage of positively stained tissue (Area %) is calculated by dividing positive stained NovaRed pixels by the total amount of grey scale pixels representing total tissue area (formula 1):

$$\text{Formula 1: Area (\%)} = \frac{\text{Number of pixels positive for NovaRed}}{\text{number of pixels in total tissue}} \times 100$$

The mean intensity was calculated following the protocol described previously by Nguyen (18). Hereby, the mean intensity represents the chromogen intensity that is proportional to the expression/level of protein (18). The pixel intensities of separated NovaRed images range from 0 to 255 in Fiji/ImageJ software, where the value 0 represents the darkest shade of the color, whereas 255 represents the lightest shade of color in the image. Hereby, it should be remembered that the darker the positive NovaRed pixels are, the smaller their intensities are. Thus, the reciprocal intensity is calculated by subtracting the value obtained by dividing the total number of NovaRed pixels by the area of positive NovaRed staining from 255 (formula 2). The reciprocal intensity is defined as the mean intensity and is proportional to the amount of positive NovaRed pixels present in the analyzed image.

$$\text{Formula 2: Mean intensity} = 255 - \frac{\text{Sum of intensities of pixels positive NovaRed}}{\text{Total number of pixels positive for NovaRed}}$$

Data analyses were performed using R software V.4.0.0 (Boston, MA).

Statistical Analysis of Immunohistochemical Staining

Linear regression and linear mixed model analyses with a random effect on intercept, correcting for sex and smoking status, were performed to determine the association between age and each stained ECM protein using SPSS software V.27 (IBM Corp. in Armonk, NY). $P < 0.05$ was considered significant.

RESULTS

Patient Characteristics

The clinical characteristics of the control patients included in the transcriptomics data set are depicted in Table 1 and included 192 ex-smokers and 78 current smokers with a normal lung function and an age range of 37–80 yr. The clinical characteristics of the proteomics data set are depicted in Table 2 and included nine ex-smoking controls with normal lung function and an age range of 49–76 yr.

The clinical characteristics of the 62 control patients used for IHC staining are summarized in Table 3. Forty-two lung tissues were collected in Groningen and included 14 never-smokers, 18 ex-smokers, and 10 current smokers. The 20 lung tissues collected in Rochester were all derived from never smokers.

Gene Expression Signature for Lung Aging in Nondisease Controls

To determine the association between age and ECM gene expression, we first assessed the age-associated gene expression differences in the nondisease control lung tissues. In total, 4,201 probes corresponding to 4,147 unique genes were significantly associated with age; of which 2,247 probes coding for 2,226 genes showed a higher and 1,954 probes coding for 1,939 genes a lower gene expression with higher age (full list in Supplemental File S1). Collagen type XVI α 1 (*COL16A1*), Ectodysplasin A2 Receptor (*EDA2R*), and Polypeptide N-acetylgalactosaminyltransferase 6 (*GALNT6*) were the top three most significantly higher expressed genes with increasing age, whereas γ-glutamylcyclotransferase (*GGCT*), Calmodulin Regulated Spectrin Associated Protein Family Member 3 (*KIAA1543*), and Zinc Finger Protein 518B (*ZNF518B*) the top three most significantly lower expressed in nondisease control patients. The top 10 most significantly higher and lower expressed genes are depicted in Table 4.

Enrichment of Matrisome Pathway among the Age-Associated Gene Signature in the Lung Tissue

As we were specifically interested in age-associated differences in ECM gene expression, we next assessed the enrichment of the ECM genes among the ranked gene list using GSEA analysis for the Matrisome geneset consisting of 1026 ECM (-associated) genes of which 915 were present in our data.

The GSEA analysis showed a strong, significant positive enrichment of the Matrisome pathway [(enrichment score of 0.387) Fig. 2] with a total of 318 core enriched ECM genes.

Table 3. *Patient characteristics immunohistochemistry staining*

	Groningen	Rochester
Number, *N*	42	20
Age, years, median (range)	61 (21–82)	51 (18–80)
Male/female, *N*	15/27	5/15
Never-smoker, *N*	14	20
Ex-smoker, *N*	18	0
Current smoker, *N*	10	0
FEV_1, means ± SE	101 ± 15.46	NA
FEV_1/ FVC ratio, means ± SE	0.76 ± 0.05	NA

The FEV_1 and FVC data were not available for lung tissues from Rochester and for few cases from Groningen. FEV_1: forced expiratory volume in 1 s, FVC: forced vital capacity, NA: not applicable.

Table 4. *The top 10 genes with higher and lower expression in relation to age in nondisease control lung tissue*

Genes Higher Expressed with Higher Age				Genes Lower Expressed with Higher Age			
Probe Number	Gene Name	Meta Summary	Adjust BH	Probe Number	Gene Name	Meta Summary	Adjust BH
26059	*COL16A1*	0.012	1.08E-15	44483	*GGCT*	−0.007	4.26E-10
27901	*EDA2R*	0.025	1.02E-14	27529	*KIAA1543*	−0.010	2.72E-09
11226	*GALNT6*	0.013	2.63E-14	43729	*ZNF518B*	−0.010	4.18E-09
23264	*MXRA8*	0.001	1.38E-13	26110		−0.012	1.93E-07
26591	*LOXL1*	0.016	1.35E-12	1257		−0.006	3.48E-07
46136	*NFASC*	0.014	5.93E-12	5658	*FANCE*	−0.009	9.38E-07
36412		0.013	8.85E-12	30969	*TMEM41B*	−0.006	1.98E-06
18268	*ITGBL1*	0.022	1.41E-11	4655	*EFNA1*	−0.009	2.97E-06
17176	*MMP2*	0.011	2.15E-11	44483	*GGCT*	−0.012	3.41E-06
16116	*F8*	0.023	4.69E-11	27529	*KIAA1543*	−0.007	4.70E-06

The top 25 most significant core enriched ECM (-associated) genes are shown in Table 5 (full list in Supplemental File S2).

ECM Proteins Are among the Top Ranked Age-Associated Proteins in Lung Tissue

Next, we determined the association between age and protein levels in the lung in the proteomic data set. We identified 25 differentially expressed proteins, including 20 proteins of which levels were higher with higher age and five proteins of which the levels were lower with higher age (Fig. 3). Among the 20 proteins with higher protein levels with higher age were several ECM proteins including COL1A1, COL6A1, COL6A2, COL14A1, FBLN2, LTBP4, and LUM.

Overlap in Age-Associated ECM Proteins in Lung Tissue on Transcript and Protein Level

Next, we determined the overlap between the age-associated ECM genes identified in the transcriptomic analysis and the age-associated proteins in the proteomic analysis. We identified seven ECM proteins that were significantly associated with age with correlation in the same direction in both datasets, i.e., higher levels with higher age. This included COL1A1, COL6A1, COL6A2, COL14A1, FBLN2, LTBP4, and LUM (Fig. 4*A*). The β values for the age association of the seven age-associated ECM genes from the transcriptomics analysis are shown in the forest plot (Fig. 4*B*). The seven overlapping age-associated ECM proteins were among the top eight proteins in the proteomics analysis (Fig. 3).

Localization of Age-Associated ECM Proteins in Lung Tissue

The immunohistochemically stained tissues were assessed for the localization of the age-associated ECM proteins in the lung (Fig. 5). All ECM proteins including COL1A1, COL6A1, COL6A2, COL14A1, FBLN2, LTBP4, and LUM showed positive staining in the parenchyma. The collagens COL1A1, COL6A1, and COL6A2, as well as FBLN2, showed positive staining in the submucosa and adventitia of the airway wall, and in the adventitia of the blood vessel. In addition, FBLN2 staining was also present in the wall of small vessels. The localization of FBLN2 is suggestive of colocalization with elastin (19). Interestingly, COL14A1 showed positive staining in the airway adventitia, airway smooth muscle (ASM) layer, and the apical region of the bronchial epithelium and macrophages. In the blood vessels, COL14A1 was localized in the endothelium and partly in the smooth muscle layer. LTBP4 staining was most prominent in blood vessel smooth muscle and was also

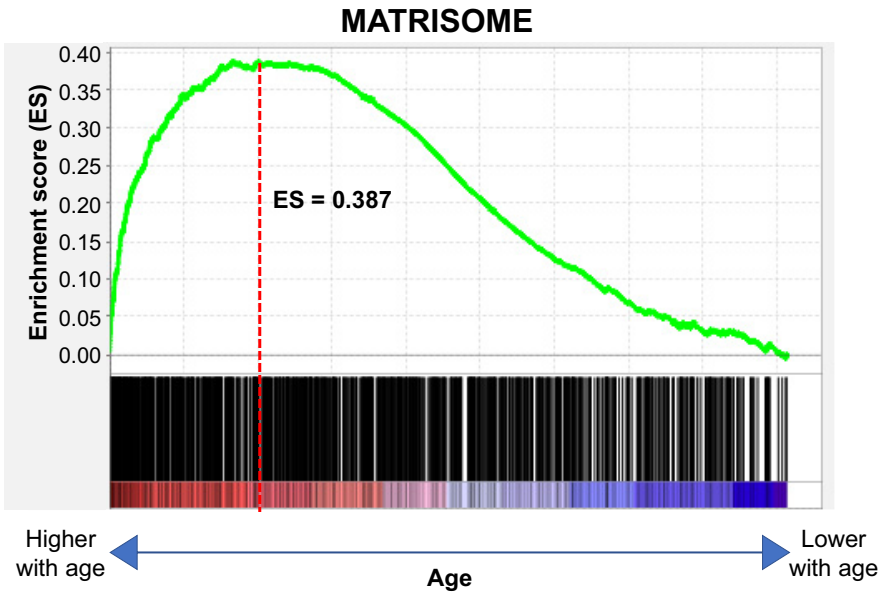

Figure 2. Enrichment of Matrisome pathway among the age-associated gene signature in nondisease control lung tissue. The vertical black bar indicates the position and green curve indicates the height of the enrichment score of a specific gene of the Matrisome. Genes are ranked from the highest to the lowest expressed (from *left* to *right*) with increasing age. The red dotted line indicates the enrichment score (0.387) of the Matrisome with increasing age.

Table 5. *GSEA analysis revealed the association of ECM gene expression in nondisease control lung tissue with aging*

Gene Symbol	Rank in Gene List	Rank Metric-Score	Running ES	Core Enrichment
COL16A1	1	9.26	0.006	Yes
LOXL1	3	8.25	0.010	Yes
MMP2	6	7.85	0.015	Yes
FRZB	8	7.60	0.020	Yes
LTBP2	12	7.39	0.024	Yes
COL1A1	14	7.33	0.028	Yes
DPT	19	7.10	0.032	Yes
LTBP1	26	6.88	0.036	Yes
SDC3	33	6.72	0.040	Yes
COL1A2	35	6.62	0.044	Yes
HTRA1	41	6.48	0.047	Yes
AEBP1	44	6.42	0.051	Yes
COL6A1	57	6.18	0.054	Yes
C1QTNF7	65	6.03	0.057	Yes
ECM2	74	5.84	0.060	Yes
WNT10A	75	5.84	0.064	Yes
COL3A1	85	5.77	0.067	Yes
SPARC	86	5.76	0.070	Yes
LOXL4	97	5.64	0.073	Yes
ITIH3	111	5.53	0.076	Yes
SPON1	114	5.502	0.079	Yes
CTHRC1	118	5.45	0.082	Yes
COL6A2	122	5.42	0.085	Yes
PLXNB1	124	5.38	0.088	Yes
SMOC2	129	5.32	0.091	Yes

The top 25 ranked enriched ECM genes. ES, enrichment score.

present in the bronchial epithelium, ASM layer, and macrophages. LUM staining was present in the bronchial epithelium, ASM layer, endothelium, and blood vessel smooth muscle layer. An overview of the strength and localization of the positive stained age-associated ECM proteins in different compartments of the lung is summarized in Table 6.

Evaluation of Age-Associated ECM Protein Differences in Lung Tissue Using Immunohistochemistry

Following the localization of the seven age-associated ECM proteins in lung tissue, we determined the age-association in whole lung tissue and in different lung regions, i.e., parenchyma, airway wall, bronchial epithelium, and vessel walls with respect to the percentage of positive stained tissue area as well as the mean intensity of the positive staining. No staining was detected in the negative controls, images are included in Supplemental File S3.

Age Association of COL6A2 Staining in Whole Lung Tissue

Analysis of the whole tissue showed a significantly positive association between age and the mean intensity of the COL6A2 (Fig. 6*A*) positive stained tissue, but not for its percentage area. No age-association was found for COL1A1, COL6A1, COL14A1, FBLN2, LTBP4, and LUM positive staining in whole lung tissue.

Age Association of COL1A1 and COL6A2 Staining in Lung Parenchyma

The analysis of the parenchymal regions showed a significantly positive association between age and the mean intensity of COL1A1 and COL6A2 positive stained parenchymal tissue (Fig. 6*B*), but no association was found for the percentage area stained. No associations were found between age and COL6A1, COL14A1, FBLN2, LTBP4, and LUM positive stained parenchymal tissue.

Age Association of COL6A2 Staining in the Airway Wall

The airway wall was analyzed for the percentage area and mean intensity of COL1A1, COL6A1, COL6A2, COL14A1, FBLN2, LTBP4, and LUM positive staining. Age was significantly positively associated with the mean intensity of COL6A2 in the airway wall. (Fig. 6*C*). However, no age-associated difference was observed for the percentage area of COL1A1, COL6A1 COL6A2, COL14A1, FBLN2, LTBP4, and LUM, and the mean intensity of COL1A1, COL6A1, COL14A1, FBLN2, LTBP4, and LUM positive staining.

Age Association of COL14A1 Staining in the Bronchial Epithelium

COL14A1, LTBP4, and LUM showed positive staining in the bronchial epithelium and were therefore analyzed for their association with age. The percentage area of COL14A1 was positively associated with age (Fig. 6*D*). No age association was observed for percentage area and mean intensity of LTBP4 and LUM, and mean intensity of COL14A1 positive staining in the bronchial epithelium.

Age Association of ECM Staining in the Blood Vessel

The blood vessel wall was analyzed for the percentage area and mean intensity of COL1A1, COL6A1, COL6A2, COL14A1, FBLN2, and LTBP4 positive staining. For LUM, the region from tunica media to endothelium of the blood vessel was analyzed. The mean intensity of COL6A2 staining in blood vessel walls showed a significant positive association with age (Fig. 6*E*), whereas the mean intensity of COL1A1 staining in the blood vessel walls showed a negative association with increasing age (Fig. 6*E*). The percentage area of COL1A1, COL6A1, COL6A2, COL14A1, FBLN2, LTBP4, and LUM positive staining; and the mean intensity of COL6A1, COL14A1, FBLN2, LTBP4, and LUM positive staining were not associated with age.

Age-Associated Differences in Subset of Never-Smokers

While our initial transcriptomic and proteomic analysis consisted of current and ex-smokers and our IHC analysis also included never-smokers, we separately analyzed the IHC images from never-smokers to investigate whether our age-associated differences were affected by smoking status. The whole lung tissue from never-smoker controls showed a positive age association for the percentage area of COL6A2 and FBLN2 and mean intensity of COL6A2 stained tissues (Fig. 7*A*), whereas with the inclusion of current and ex-smokers, only a positive age association for mean intensity of COL6A2 was found (Fig. 6*A*). The percentage area of FBLN2 and mean intensity of COL1A1 showed a positive association with age in the parenchymal region of never-smoker patients (Fig. 7*B*), whereas with the inclusion of current and ex-smokers a positive association of the mean intensity of COL1A1 and COL6A2 was found (Fig. 6*B*).

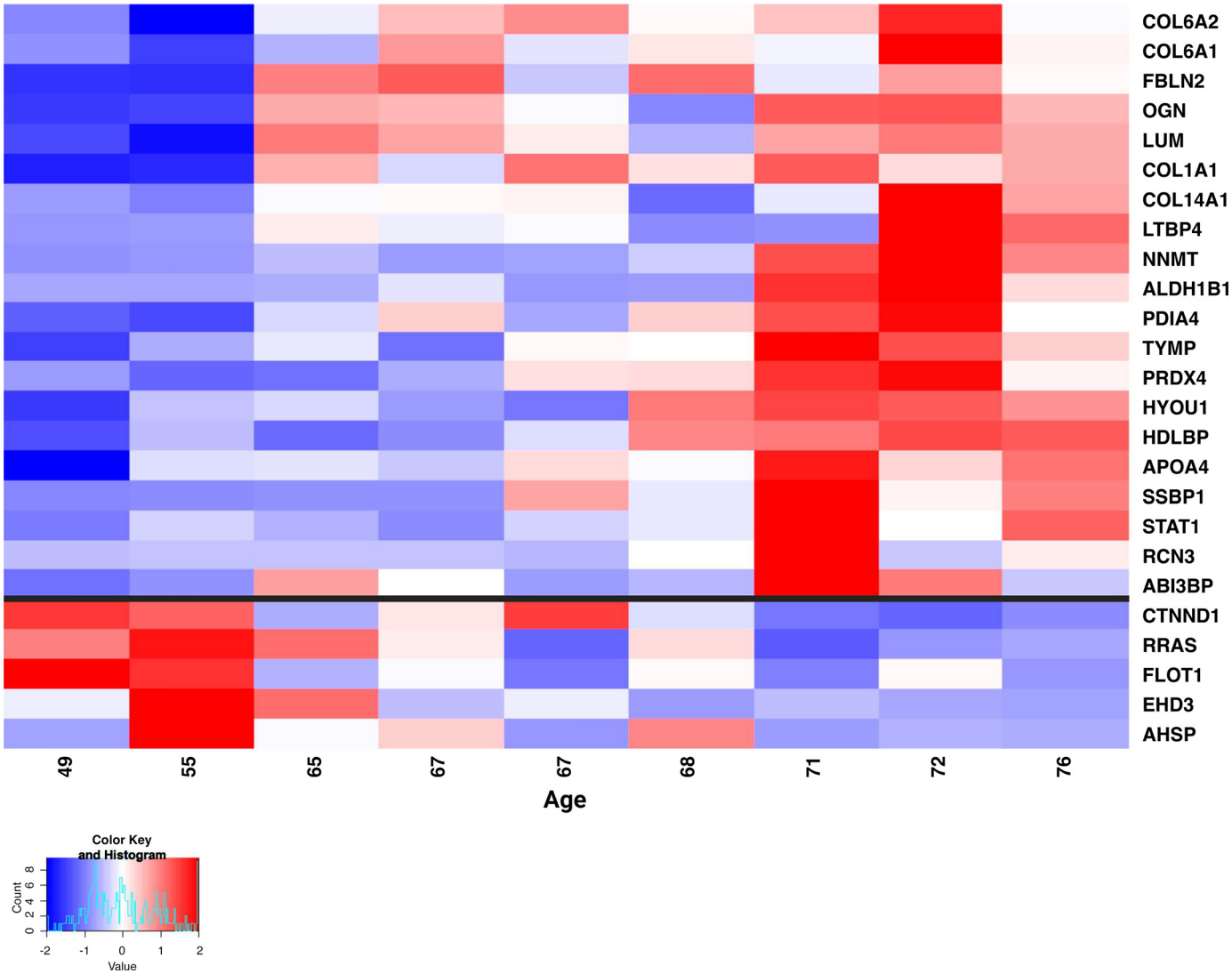

Figure 3. Heatmap of age-associated proteins in the lung of nondisease control patients. The heat map shows the results of the proteomic analysis of human lung tissue from control patients. The *upper* part of the map shows the significantly upregulated and the *lower* part the significantly downregulated proteins with age. For the statistical analysis, *P* values were corrected using the Benjamini–Hochberg (FDR) method using a threshold of 0.05. FDR, fold discovery rate.

Similar to the results of airway wall from the combined groups of never, current, and ex-smokers (Fig. 6*A*), mean intensity of COL6A2 positive stained airway wall from never-smoker control was positively associated with age (Fig. 7*C*). In contrast to the results obtained from bronchial epithelium from in all control patients (Fig. 6*D*) showing only the percentage area of COL14A1 positively associated with age, we found the percentage area and mean intensity of COL14A1 and LUM to be positively associated with age in never-smokers (Fig. 7*D*). As in the blood vessel from all control patients (Fig. 6*E*), never-smokers (Fig. 7*E*), showed a positive age-association of the mean intensity of COL6A2. However, mean intensity of COL1A1 is negatively associated with age only in blood vessels from all control patients.

Age-Associated ECM Differences Are Compartment Specific

We have summarized the results of the immunohistochemical analyses in Fig. 8, separating the analyses on the complete group from the subset of never-smokers. We only indicate the significant associations with age with the strength of the association based on the p-values. With respect to the total area of positive ECM staining, the analysis of the combined groups of never, current, and ex-smokers (Fig. 8 (1)) showed that COL6A2 was the only age-associated ECM protein with a higher level in all lung compartments including the parenchymal region (Fig. 8 (1 G)), airway wall (Fig. 8 (1H)), and blood vessel (Fig. 8 (1 J)); except in the bronchial epithelium region where it is not expressed. Compartment specific age-associated differences have been observed in the lung with a higher level of COL1A1 in the parenchyma (Fig. 8 (1 G)), whereas COL1A1 level was lower in the blood vessel (Fig. 8 (1 J)), with increasing age.

The analysis of the subset of never-smokers (Fig. 8 (2)) showed a higher spatial distribution of FBLN2 in whole tissue (Fig. 8 (2 A)) and parenchyma (Fig. 8 (2B)) and COL14A1 and LUM in the bronchial epithelium (Fig. 8 (2 D)) with increasing age. Additionally, the levels of COL14A1 and LUM

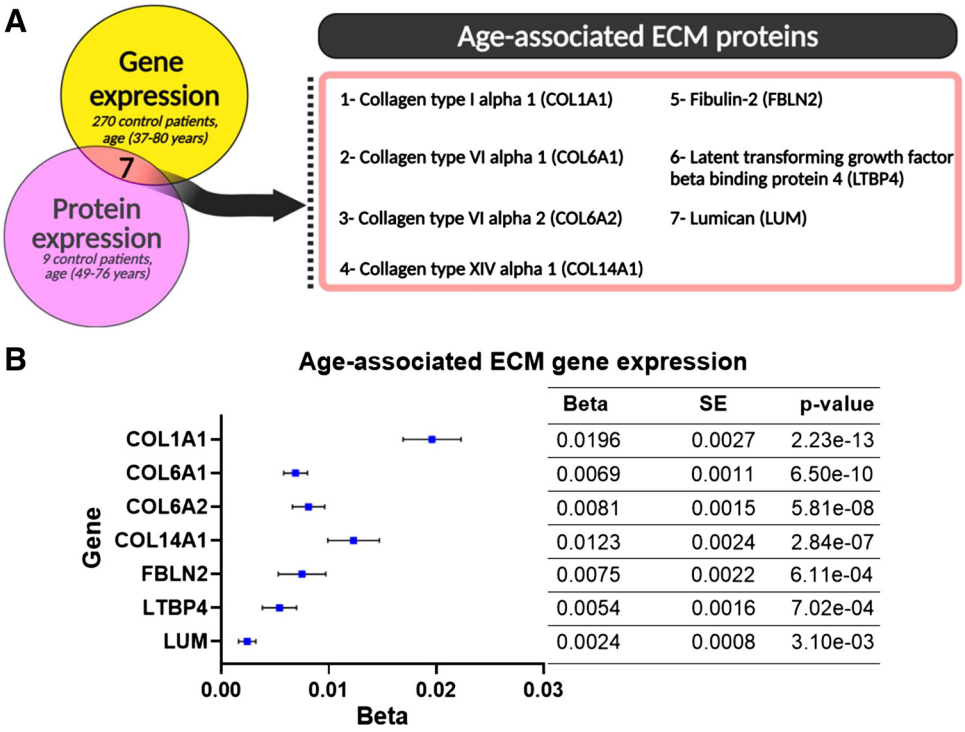

	Beta	SE	p-value
COL1A1	0.0196	0.0027	2.23e-13
COL6A1	0.0069	0.0011	6.50e-10
COL6A2	0.0081	0.0015	5.81e-08
COL14A1	0.0123	0.0024	2.84e-07
FBLN2	0.0075	0.0022	6.11e-04
LTBP4	0.0054	0.0016	7.02e-04
LUM	0.0024	0.0008	3.10e-03

Figure 4. Overlap in age-associated ECM proteins in the lung tissue on transcript and protein level. *A*: transcriptomic and proteomic results were examined for the overlapping of ECM gene and its encoded protein. Seven ECM proteins including COL1A1, COL6A1, COL6A2, COL14A1, FBLN2, LTBP4, and LUM were significantly higher with age on gene and protein level. *B*: the β-coefficients for age of the seven ECM genes overlapping with encoded ECM proteins are shown in the forest plot. For the statistical analysis, *P* values were corrected using the Benjamini–Hochberg (FDR) method using a threshold of 0.05. COL1A1, collagen type I α 1; COL6A1, collagen type VI α 1; COL6A2, collagen type VI α 2; COL14A1, collagen type XIV α 1; FBLN2, fibulin-2; LTBP4, latent transforming growth factor β binding protein 4; LUM, lumican; FDR, fold discovery rate; SE, standard error.

were higher in the bronchial epithelium (Fig. 8 (2I)) with increasing age. The level of COL6A2 was higher in whole tissue (Fig. 8 (2 F)) airway wall (Fig. 8 (2H)) and blood vessels (Fig. 8 (2 J)) with increasing age. Overall, we identified more significant age associations in the subgroup of never-smokers compared to combined groups of never, current, and ex-smokers.

DISCUSSION

Our study describes the age-associated differences in human lung ECM using transcriptomic, proteomic, and immunohistochemical analyses. Our results indicate that the human lung ECM remodels with normal aging. The Matrisome pathway, including both ECM and ECM-related proteins, was significantly and positively enriched among the age-associated gene signature in nondiseased control lung tissue. Comparing age-associated transcriptomic and proteomic differences in lung tissue, we identified seven age-associated ECM (and ECM-associated) proteins being COL1A1, COL6A1, COL6A2, COL14A1, FBLN2, LTBP4, and LUM which all showed higher levels in whole lung tissue with higher age. Subsequent immunohistochemical staining in different compartments of the lung revealed differences in the location patterns of these ECM proteins with all proteins being found in the airway wall and blood vessels and three proteins including COL14A1, LTBP4, and LUM with clear localization in the bronchial epithelium. Age-associated differences were observed in the combined groups of never, current, and ex-smokers for COL6A2 in whole tissue, parenchyma, airway wall, and blood vessels, and for COL1A1 in the parenchyma and blood vessel. The subset of never-smokers showed age associations for COL14A1 and LUM in the bronchial epithelium and COL6A2 and FBLN2 in whole tissue, airway wall, and blood vessels.

Our findings are in line with previous data showing a higher level of collagens and collagen-related proteins in the lung of 24-mo-old mice and a higher collagen deposition observed in parenchymal regions of aged mice (20). Other studies specifically showed a higher level of COL1A1, COL6A1, and COL6A2, but a lower level of COL14A1 with higher age in mouse lung tissue (21, 22).

In our study, COL6A2 was the only protein observed with a higher level throughout the different lung compartments. Surprisingly, no age-associated difference was observed for COL6A1 in any of the lung compartments where it was localized. COL6 is formed through the assemblance of three alpha chains including COL6A1, COL6A2, and COL6A3 into a triple-helix monomer in a 1:1:1 stoichiometric ratio (23). Later, the alpha chains COL6A4, COL6A5, and COL6A6 were identified and share a similar structure to COL6A3; however, the COL6A4 is not expressed in humans. The interchangeability of COL6A3 with COL6A4, COL6A5, or COL6A6 has been suggested. COL6 triple helices monomers assemble into antiparallel dimeric structures via disulfide bonds, the formed dimers align to form disulfide-bonds stabilized tetramers (23, 24). COL6 plays an important role in cell-ECM interaction, through interaction with cell surface receptors including integrins (23). In addition, COL6 enhances lung epithelial cell spreading and facilitates wound healing (24) and COL6 depletion in mice was linked to altered basement membrane structure and diminished cell-ECM interaction in the lung resulting in an altered pulmonary elasticity and less tolerance for physical exercises(23). These suggest the importance of COL6 in the mechanical regulation of the lung; however, it remains unresolved why only COL6A2 was higher expressed in our lung tissues and not COL6A1. Thus, it will be

interesting to examine the role of COL6A2 in the lung and its implication of lung aging phenomenon.

COL14A1 belongs to the collagen family of FACITs (Fibril Associated Collagens with Interrupted Triple helices) which is primarily known for its role in the organization of collagen fibrils (25). In addition, COL14A was identified as a key component in turnover and differentiation of epithelial cells (21). Angelidis et al. (22) showed a lower level of COL14A1 level

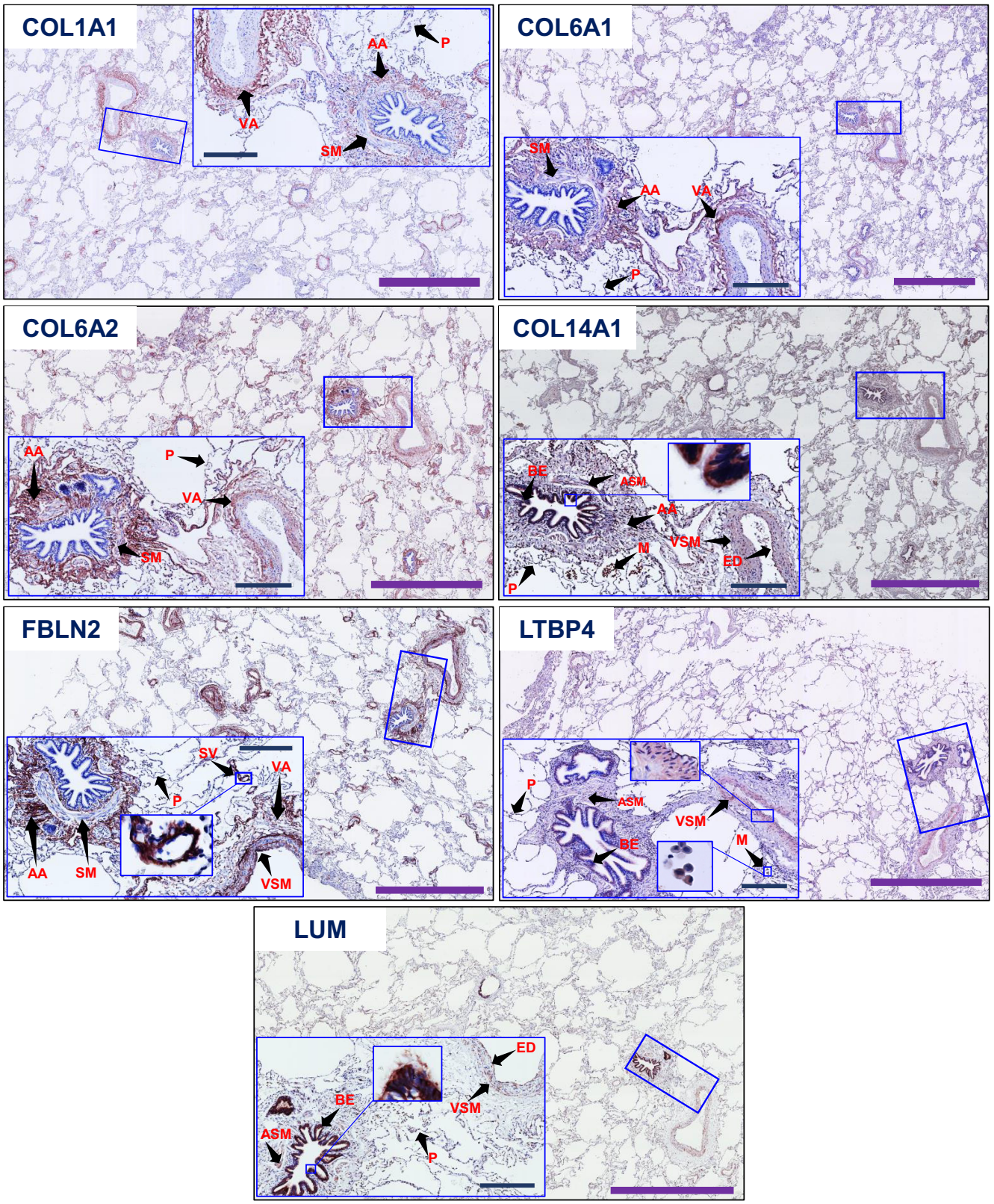

AJP-Lung Cell Mol Physiol • doi:10.1152/ajplung.00334.2022 • www.ajplung.org

Table 6. *Overview of positive stained areas for age-associated ECM proteins including COL1A1, COL6A1 COL6A2, COL14A1, FBLN2, LTBP4, and LUM and their semi-quantitative score in the lung compartments*

		Airway Wall				Blood Vessel		
ECM Protein	Parenchyma	SM	AA	ASM	Bronchial Epithelium	BA	VSM	ED
COL1A1	+	+ +	+ +	−/+	−	+ +	+	−
COL6A1	+ +	+	+ +	+	−	+ +	+	+
COL6A2	+ +	+ +	+ +	+	−	+ +	+	+ +
COL14A1	+	+	+	+ + +	+ + +	+	+ +	+ + +
FBLN2	+	+ +	+ +	−	−	+ +	+ + +	−
LTBP4	+	+	+	+ +	+	−	+ +	−
LUM	+	+	+	+ + +	+ + +	−	+ +	+ +

COL1A1, collagen type I α 1; COL6A1, collagen type VI α 1; COL6A2, collagen type VI α 2; COL14A1, collagen type XIV α 1; FBLN2, fibulin-2; LTBP4, latent transforming growth factor beta binding protein 4; LUM, lumican; AA, airway adventitia; BA, blood vessel adventitia; ED, endothelium; BE, bronchial epithelium; ASM, airway smooth muscle; VSM, blood vessel smooth muscle; SM, submucosa; (−), no staining; (+), weak staining; (+ +), medium staining; (+ + +), strong staining.

and differences in cell type composition in the bronchial epithelium of aged mice. Our study shows a higher level of COL14A1 in the bronchial epithelium in human lungs with increasing age, suggesting an attempt for the maintenance of the cell type composition in the bronchial epithelium of aged control patients. Additional investigations are needed for a better understanding of the role of COL14A1 in the bronchial epithelial layer. Higher age was also associated with higher levels of LUM in the bronchial epithelium. LUM is a small leucine-rich proteoglycan (SLRP) that is important for the regulation of biological processes including cell migration and adhesion, besides its role in collagen fibrillogenesis (26, 27). Saika et al. (26) showed that LUM expression increases in the injured mouse corneal epithelium in the earlier phase of wound healing, and the healing of epithelial injury was delayed in LUM-deficient mice compared with controls. Later, Yamanaka et al. (28) showed that LUM improved wound healing through binding to the transforming growth factor-β (TGF-β) receptor 1 (ALK5). The incidence of lung injury has been shown to be higher in the elderly. Therefore, we suggest that the higher level of LUM in the bronchial epithelium with higher age might be a response to lung injury.

Lung elasticity is known to be less with higher age. FBLN2 serves as a bridge between fibrillin and elastin molecules and has shown a strong binding affinity to tropoelastin (29). However, previous study has demonstrated that FBLN2 is dispensable for elastin fiber formation in mouse lung (30). Our study showed a higher percentage area, but not a higher level of FBLN2 in parenchyma region of never-smokers control patients. These findings indicate a possible role in the stabilization and/or maintenance of the function of elastin fibers in the parenchymal region. FBLN2 has been identified as a positive regulator of TGF-β1 activity (31, 32). FBLN2-KO mice displayed a lower level of COL1 expression in the ischemic myocardium (33). Our study shows a higher distribution of FBLN2 and a higher level of COL1A1 in the parenchymal region. However, the link between the higher level of COL1A1 and the higher percentage area of FBLN2 cannot be confirmed in our study. COL1 triple helix consists of 2 COL1A1 chains and one chain of COL1A2. The COL1 triple helices auto-assemble to form COL1 fibrils (21). COL1 contributes to the tissue tensile strength, and its increased deposition may contribute to the lung stiffening with age, as significant increases in stiffness were observed in the parenchyma of old (41–60 yr) compared with young (11–30 yr) human lung tissues (34). Surprisingly, COL1A1 level was lower in blood vessel wall with age, indicating differences in the regulation of COL1A1 expression in the blood vessel compared with the parenchyma and the importance of assessing age-associated differences in different structural compartments in the lung.

Our subgroup analysis in never-smokers showed some differences in the levels of ECM proteins compared to the combined group of never, current, and ex-smokers. The most differences were specific to the bronchial epithelium with higher levels of COL14A1 and LUM in never-smokers and to the blood vessel with lower levels of COL1A1 in the combined groups of never, current, and ex-smokers. In human arteries derived from carotid, coronary, pulmonary, or kidney, Faarvang et al. (35) demonstrated using Masson's trichrome staining and proteome analysis that the area fraction of collagen and the COL1A1 level were significantly decreased in current smokers compared with never-smoker control patients, respectively. In addition, they found no differences in COL6A1, COL6A2, COL14A1, FBLN2, and LUM levels in never-smokers compared with current smokers (35). These data suggest that the lower level of COL1A1 in the blood

Figure 5. Localization of age-associated ECM proteins in human lung tissues. Following the immunohistochemical staining the age-associated ECM proteins were localized in the lung tissue. All the stained ECM proteins including COL1A1, COL6A1, COL6A2, COL14A1, FBLN2, LTBP4, and LUM were located in the parenchyma. COL1A1, COL6A1, and COL6A2 were localized to the submucosa and airway adventitia and blood vessel adventitia. COL14A1 is localized to the ASM layer, bronchial epithelium, endothelium, blood vessel smooth muscle layer and macrophages. FBLN2 is also present in the submucosa and airway adventitia, smooth muscle layer of large blood vessel, and in the wall of small vessel. LUM and LTBP4 are both present in the bronchial epithelium, airway wall and blood vessel smooth muscle. Macrophages were also positive for LTBP4 staining, whereas LUM was localized to the ASM layer. Arrows indicate areas of positive staining. These stainings were performed individually for the 64 lung tissues from control patients, which explain the variation observed in the intensity of hematoxylin staining. Blue Scale bar 300 μm and purple scale bar 2 mm. COL1A1, collagen type I α 1; COL6A1, collagen type VI α 1; COL6A2, collagen type VI α 2; COL14A1, collagen type XIV α 1; FBLN2, fibulin-2; LTBP4, latent transforming growth factor β binding protein 4; LUM, lumican; AA, airway adventitia; BA, blood vessel adventitia; ED, endothelium; BE, bronchial epithelium; ASM, airway smooth muscle; VSM, blood vessel smooth muscle; SM, submucosa; SV, small vessel; M, macrophage; P, parenchyma.

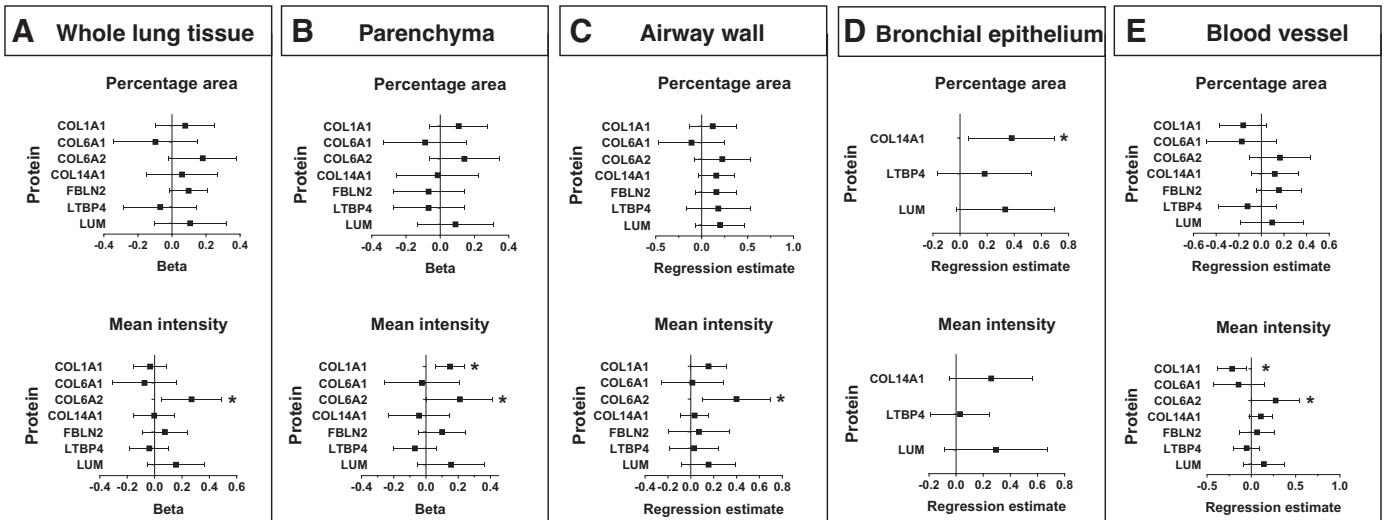

Figure 6. Forest plot of beta and regression estimates for age of the percentage area and mean intensity of age-associated ECM proteins in the whole lung tissue, parenchyma, airway wall, bronchial epithelium, and blood vessel from combined groups of never-smokers, current smokers, and ex-smokers. Lung tissue sections form all control patients without airflow limitation aged from 18 to 82 yr were immunohistochemically stained for the seven age-associated ECM proteins and the positive staining was analyzed using Image J software for the percentage area and mean intensity for COL1A1, COL6A1, COL6A2, COL14A1, FBLN2, LTBP4, and LUM positive staining. Hereby, the whole lung tissue and derived lung compartments including parenchyma, airway wall, bronchial epithelium and blood vessel were analyzed separately. The analysis of whole lung tissue (*A*) showed a positive association of mean intensity of COL6A2 (*N* = 61) positive stained tissue with age, but no association for percentage area of COL6A2. The percentage area and mean intensity of COL1A1 (*N* = 62), COL6A1 (*N* = 62), COL14A1 (*N* = 60), FBLN2 (*N* = 62), LTBP4 (*N* = 62), and LUM (*N* = 62) positive stained tissue showed no association with age. The analysis of the parenchyma (*B*) revealed the positive association of mean intensity of COL1A1 (*N* = 61) and COL6A2 (*N* = 61) positive stained tissue with age, but no association was found for the percentage area. Both mean intensity and percentage area of COL6A1 (*N* = 62), COL14A1 (*N* = 60), FBLN2 (*N* = 62), LTBP4 (*N* = 62), and LUM (*N* = 62) positive stained tissues showed no association with age. In the airway wall (*C*), age was positively associated with the mean intensity of COL6A2 (*N* = 219), but not with percentage area of COL6A2. The percentage area and mean intensity of COL1A1 (*N* = 252), COL6A1 (*N* = 240), COL14A1 (*N* = 224), FBLN2 (*N* = 240), LTBP4 (*N* = 230), and LUM (*N* = 231) positive stained tissue showed no association with age. In the bronchial epithelium (*D*), age was positively associated with the percentage area of COL14A1 (*N* = 224), but not with mean intensity of COL14A1. There was no age-association with the percentage area and mean intensity of LTBP4 (*N* = 214) and LUM (*N* = 234) positive stained tissues. The age-associated ECM proteins COL1A1, COL6A1, COL6A2, and FBLN2 were not expressed in the bronchial epithelium. The blood vessel (*E*) showed a positive association between age and the mean intensity of COL6A2 (*N* = 273), but not its percentage area. Age was negatively associated with the mean in intensity of COL1A1 (*N* = 305) but not its percentage area. The percentage area and mean intensity of COL6A1 (*N* = 284), COL14A1 (*N* = 257), FBLN2 (*N* = 289), LTBP4 (*N* = 263), and LUM (*N* = 278) positive stained tissue showed no association with age. As statistical analysis, the linear regression model adjusted for sex and smoking was performed in SPSS software V.27 was used for whole lung tissue and parenchyma. For airway wall, bronchial epithelium and blood vessel, a linear mixed model adjusted for sex and smoking was applied and the regression estimate and 95% confidence intervals for age were represented for each percentage area/mean intensity. COL1A1, collagen type I α 1; COL6A1, collagen type VI α 1; COL6A2, collagen type VI α 2; COL14A1, collagen type XIV α 1; FBLN2, fibulin-2; LTBP4, latent transforming growth factor β binding protein 4; LUM, lumican; *N*, number of tissues used for each analysis. *Significant.

vessel of the combined groups of never, current, and ex-smokers is possibly linked to smoking, as the subset of only never-smokers did not show a significantly lower level of COL1A1. Woenckhaus et al. (36) showed that the mRNA level of COL14A1 was lower in the bronchial epithelium of smokers compared with the non-smokers patients. In addition, the exposure of PC3 epithelial cells to cigarette smoke also led to the downregulation of COL14A1 expression (37). Thus, our results and the literature suggest a potential effect of smoking on ECM production in the lung with increasing age.

The expression of age-associated ECM proteins in different lung compartments may occur through the activation of specific biological processes in certain cell types including fibroblasts, myofibroblasts, and ASM, which are recognized as the principal sources of ECM proteins. An increased proportion of fibroblasts was found in aged human lungs compared with the proportion of epithelial cells (3, 38) and our previous work demonstrated a link between cellular senescence and ECM dysregulation in COPD lung fibroblasts. In addition, senescent ASM displayed a higher expression of ECM proteins with higher age (39). These observations suggest that the observed age-associated differences in the lung ECM may be associated with more cellular senescence in the aged lung. Further research is needed to disentangle the mechanisms behind this and determine whether senescence could be driving the age-associated ECM changes in the lung.

We used a unique approach to assess age-associated ECM differences on levels and in specific lung compartments including the whole tissue transcript and protein analysis followed by extensive, immunohistochemical analyses in specific lung regions. Sensitivity and specificity of the antibodies as well as differences in the epitope region recognized by the antibodies may explain the differences observed in results obtained from immunohistochemical analysis compared with the proteomic analysis. The differences observed in percentage area/spatial distribution and mean intensity/level of the positive stained age-associated ECM proteins provide different information about the distribution and amount of protein present within the tissues.

Our study also had some limitations, namely, the relatively small number of nine control patients used for the proteomic analysis compared with the numbers of control

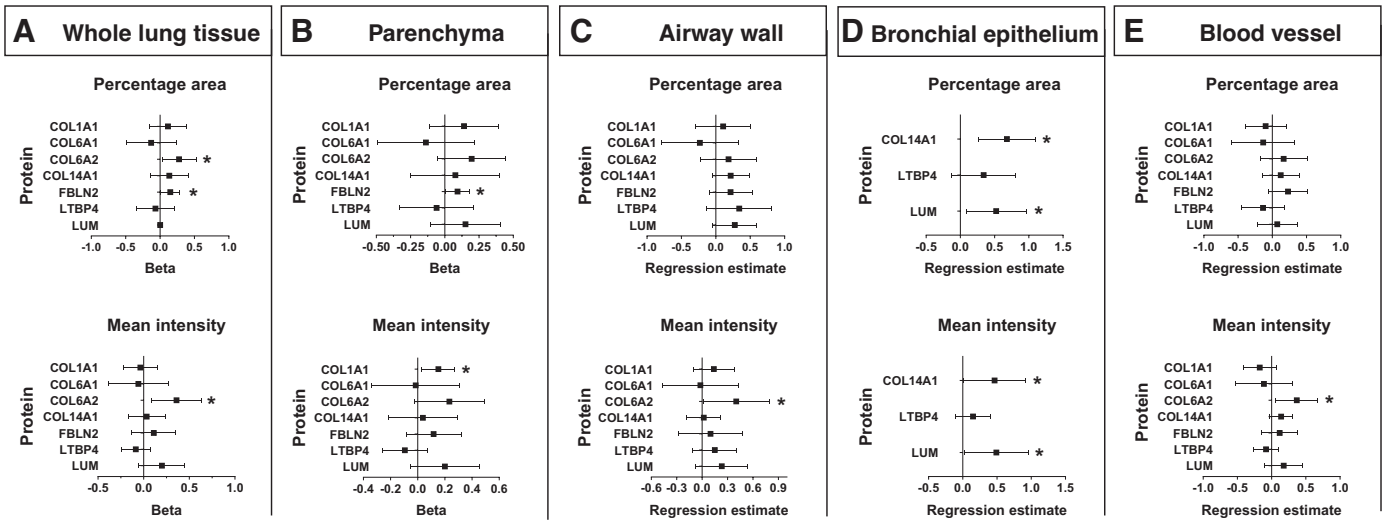

Figure 7. Forest plot of beta and regression estimates for age of the percentage area and mean intensity of age-associated ECM proteins in the whole lung tissue, parenchyma, airway wall, bronchial epithelium, and blood vessel from never-smoker control patients. Lung tissue sections from all control patients without airflow limitation aged from 18 to 82 yr were immunohistochemically stained for the seven age-associated ECM proteins and the positive staining was analyzed using Image J software for the percentage area and mean intensity for COL1A1, COL6A1, COL6A2, COL14A1, FBLN2, LTBP4, and LUM positive staining. Hereby, the whole lung tissue and derived lung compartments including parenchyma, airway wall, bronchial epithelium, and blood vessel were analyzed separately. The analysis of whole lung tissue (*A*) showed a positive association of percentage area and mean intensity of COL6A2 (*N* = 32) positive stained tissue with age. The percentage area of FBLN2 (*N* = 33) positive stained tissue showed a positive association with age, but not mean intensity of FBLN2. The percentage area and mean intensity of COL1A1 (*N* = 33), COL6A1 (*N* = 33), COL14A1 (*N* = 33), LTBP4 (*N* = 33), and LUM (*N* = 33) positive stained tissue showed no association with age. The analysis of the parenchyma (*B*) revealed the positive association of mean intensity of COL1A1 (*N* = 32) and percentage area of FBLN2 (*N* = 33) positive stained tissue with age, but no association was found for the percentage area of FBLN2 and mean intensity COL1A1. Both mean intensity and percentage area of COL6A1 (*N* = 33), COL6A2 (*N* = 32), COL14A1 (*N* = 32), LTBP4 (*N* = 33), and LUM (*N* = 33) positive stained tissues showed no association with age. In the airway wall (*C*), age was positively associated with the mean intensity of COL6A2 (*N* = 120), but not with percentage area of COL6A2. The percentage area and mean intensity of COL1A1 (*N* = 142), COL6A1 (*N* = 131), COL14A1 (*N* = 129), FBLN2 (*N* = 126), LTBP4 (*N* = 117), and LUM (*N* = 120) positive stained tissue showed no association with age. In the bronchial epithelium (*D*), age was positively associated with the percentage area and mean intensity of COL14A1 (*N* = 131) and LUM (*N* = 121) of positive stained tissues. There was no age-association with the percentage area and mean intensity of LTBP4 (*N* = 112) positive stained tissues. The age-associated ECM proteins COL1A1, COL6A1, COL6A2, and FBLN2 were not expressed in the bronchial epithelium. The blood vessel (*E*) showed a positive association between age and the mean intensity of COL6A2 (*N* = 112), but not its percentage area. The percentage area and mean intensity of COL1A1 (*N* = 148), COL6A1 (*N* = 122), COL14A1 (*N* = 112), FBLN2 (*N* = 131), LTBP4 (*N* = 107), and LUM (*N* = 121) positive stained tissue showed no association with age. As statistical analysis, the linear regression model adjusted for sex and smoking was performed in SPSS software V.27 was used for whole lung tissue and parenchyma. For airway wall, bronchial epithelium and blood vessel, a linear mixed model adjusted for sex and smoking was applied and the regression estimate and 95% confidence intervals for age were represented for each percentage area/mean intensity. COL1A1, collagen type I α 1; COL6A1, collagen type VI α 1; COL6A2, collagen type VI α 2; COL14A1, collagen type XIV α 1; FBLN2, fibulin-2; LTBP4, latent transforming growth factor β binding protein 4; LUM, lumican; *N*, number of tissues used for each analysis. *Significant.

patients, 270 and 62, used for transcriptomic analysis and immunohistochemical analysis, respectively. In addition, our study is cross sectional and therefore makes it difficult to infer any causal relationship.

As previously mentioned, the aging lung is characterized by structural and physiological alterations. As the ECM regulates different biomechanical properties of tissue and organs, and comprises key proteins responsible for lung stiffness, elasticity, and recoil. In addition, the different ECM proteins play a role in the binding and release of specific cytokines and chemokines. Therefore, the age-associated ECM differences that we showed with differences in several collagens as well as FBLN2, which co-localizes within the elastic fibers, are likely important contributors to structural and physiological changes in the aging lung.

In summary, our study revealed age-associated differences in the lung ECM from histologically normal lungs from patients with normal lung function and no history of chronic lung disease. Higher COL6A2 level with higher age was present in all lung compartments except in the bronchial epithelium, where it is not expressed. Most differences were observed in the subset of never-smokers. These ECM differences may affect lung structure and physiology with aging and as such help in understanding the development and progression of chronic lung diseases. Identifying the mechanisms regulating the ECM deposition in the aging lung will lay a strong foundation for the identification of potential triggers for the development of age-associated chronic lung diseases.

DATA AVAILABILITY

Data will be made available upon reasonable request.

SUPPLEMENTAL DATA

Supplemental File S1, File S2, and File S3: https://doi.org/10.6084/m9.figshare.21257808.v5.

ACKNOWLEDGMENTS

The stainings of COL1A1, COL6A1, COL6A2, COL14A1, FBLN2, LTBP4, and LUM on lung tissue performed in this manuscript

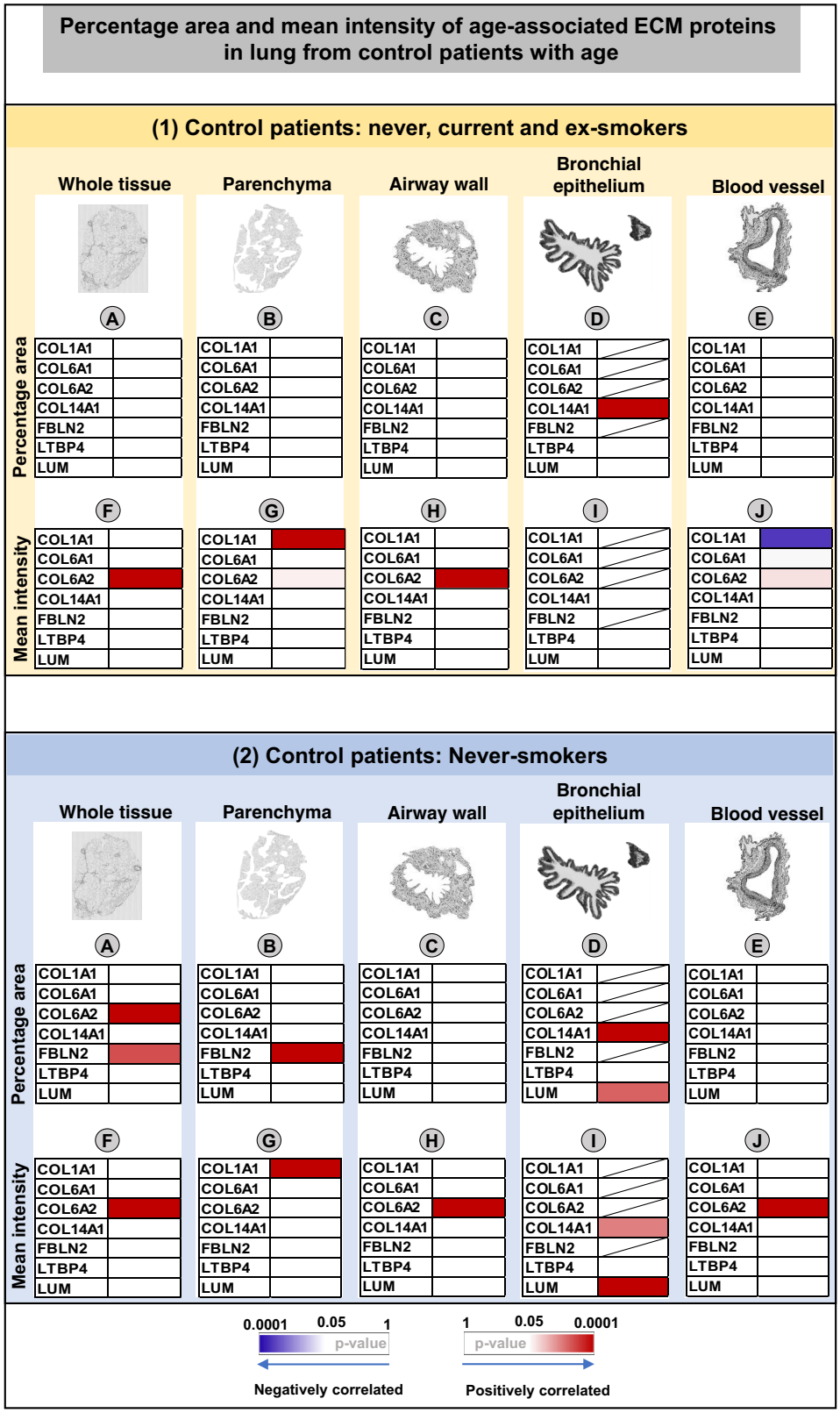

Figure 8. Summary of percentage area and mean intensity of the positive staining of age-associated ECM proteins in different compartments of the lung. For a better visualization of the results, we re-presented the p-values of results obtained from the combined groups of never, current, and ex-smokers (1) and the subset of never-smoker control patients (2) in one figure. For combined groups of never, current, and ex-smokers, the results are presented as percentage area of ECM proteins in whole tissue (1 A), parenchyma (1 B), airways wall (1 C), bronchial epithelium (1 D), blood vessel (1 E), and mean intensity in whole tissue (1 F), parenchyma (1 G), airways wall (1 H), bronchial epithelium (1 I), and blood vessel (1 J). For the subset of never-smokers, the results are presented as percentage area of ECM proteins in whole tissue (2 A), parenchyma (2 B), airways wall (2 C), bronchial epithelium (2 D), blood vessel (2 E) and mean intensity in whole tissue (2 F), parenchyma (2 G), airways wall (2 H), bronchial epithelium (2 I), and blood vessel (2 J). The combined groups of never, current, and ex-smokers showed a clear positive correlation of mean intensity of COL6A2 with age in whole tissue (1 F), parenchyma (1 G), airway wall (1H), and blood vessel (1 J). Mean intensity of COL1A1 was positively correlated with age in the parenchyma (1 G), but negatively correlated in the blood vessel (1 J). Only percentage area of COL14A1 showed an age-association in the bronchial epithelium (1 D). The never-smoker subset showed age-association for the mean intensity of COL6A2 in whole tissue (2 A), airway wall (2 H) and blood vessel (2 J), but not in the parenchyma (2 G). The percentage area and mean intensity of COL14A1 and LUM were positively correlated with age in the bronchial epithelium (2 D and 2 I). Mean intensity of COL1A1 was positively correlated with age exclusively in the parenchyma (2 G). Additionally, percentage area of COL6A2 was positively correlated with age in the whole tissue (2 A) and percentage area of FBLN2 was also positively correlated in whole tissue (2 A) and parenchyma (2 B). COL1A1, collagen type I α 1; COL6A1, collagen type VI α 1; COL6A2, collagen type VI α 2; COL14A1, collagen type XIV α 1; FBLN2, fibulin-2; LTBP4, latent transforming growth factor β binding protein 4; LUM, lumican.

were conducted as part of the HOLLAND (HistopathOLogy of Lung Aging aNd COPD) project. The HOLLAND project was initiated and supervised by Corry-Anke Brandsma, Wim Timens, and Janette Burgess, technical support was provided by Marjan Reinders-Luinge, Anja Bakker, and Theo Borghuis, and image analysis pipelines were developed by Theo Borghuis, Maunick Lefin Koloko Ngassie, and Niek Bekker. Preprint is available at https://doi.org/10.1101/2022.06.16.496465.

GRANTS

This study was partly supported by an Abel Tasman Talent Program Fellowship, in association with the Healthy Aging Alliance, provided by the University Medical Center Groningen and the Mayo Clinic, Rosalind Franklin Fellowship provided by the University of Groningen and the European Union, Stichting De Cock-Hadders grant provided by University Medical Center Groningen, NIH Grants R01 HL088029 and R01 HL0142061. The proteomics analysis was supported by the Netherlands X-omics Initiative (NWO, project 184.034.019).

DISCLOSURES

C.-A. Brandsma received research grants from Genentech. J. K. Burgess received unrestricted research funds from Boehringer Ingelheim. She has been awarded the President Netherlands Matrix Biology Society (unpaid), National Board Member Netherlands Respiratory Society (unpaid), and Assembly of Respiratory Structure and Function, American Thoracic Society, Assembly Chair (unpaid). R. Gosens received grants paid to his institution from Boehringer Ingelheim, Aquilo, and Sanofi-Genzyme. D. D. Sin received honoraria for COPD talk (Boehringer Ingelheim, AstraZeneca, GSK). W. Timens received consulting fees from Merck Sharp Dohme, and Bristol-Myers-Squibb. He is the board member of Dutch Society of Pathology and member of the Council for Research and Innovation of the Federation of Medical Specialists. None of the other authors has any conflicts of interest, financial or otherwise, to disclose.

AUTHOR CONTRIBUTIONS

M.L.K.N., R.G., Y.S.P., J.K.B., and C.-A.B. conceived and designed research; M.L.K.N., M.D.V., T.B., P.H., and J.J.T., performed experiments; M.L.K.N., M.D.V, T.B., D.D.S., P.H., and J.M.V. analyzed data; M.L.K.N., W.T., J.M.V., R.G., Y.S.P., J.K.B., and C.B. interpreted results of experiments; M.L.K.N., M.D.V., W.T., and P.H. prepared figures; M.K. drafted manuscript; M.L.K.N., M.D.V., T.B., W.T., D.D.S., D.N., P.J., P.H., G.M.-V., J.J.T., J.M.V., R.G., Y.S.P., J.K.B., and C.-A.B. edited and revised manuscript; M.L.K.N., M.D.V., T.B., W.T., D.N., P.J., P.H., G.M.-V., J.M.V., R.G., Y.S.P., J.K.B., and C.-A.B. approved final version of manuscript.

REFERENCES

1. **Zhou Y**, **Horowitz JC**, **Naba A**, **Ambalavanan N**, **Atabai K**, **Balestrini J**, **Bitterman PB**, **Corley RA**, **Ding B-S**, **Engler AJ**, **Hansen KC**, **Hagood JS**, **Kheradmand F**, **Lin QS**, **Neptune E**, **Niklason L**, **Ortiz LA**, **Parks WC**, **Tschumperlin DJ**, **White ES**, **Chapman HA**, **Thannickal VJ.** Extracellular matrix in lung development, homeostasis and disease. *Matrix Biol* 73: 77–104, 2018. doi:10.1016/j.matbio.2018.03.005.
2. **Meiners S**, **Eickelberg O**, **Königshoff M.** Hallmarks of the ageing lung. *Eur Respir J* 45: 807–827, 2015. doi:10.1183/09031936.00186914.
3. **Cho SJ**, **Stout-Delgado HW.** Aging and lung disease. *Annu Rev Physiol* 82: 433–459, 2020. doi:10.1146/annurev-physiol-021119-034610.
4. **Copley SJ**, **Wells AU**, **Hawtin KE**, **Gibson DJ**, **Hodson JM**, **Jacques AE**, **Hansell DM.** Lung morphology in the elderly: comparative CT study of subjects over 75 years old versus those under 55 years old. *Radiology* 251: 566–573, 2009. doi:10.1148/radiol.2512081242.
5. **Brandenberger C**, **Mühlfeld C.** Mechanisms of lung aging. *Cell Tissue Res* 367: 469–480, 2017. doi:10.1007/s00441-016-2511-x.
6. **Huang K**, **Rabold R**, **Schofield B**, **Mitzner W**, **Tankersley CG.** Age-dependent changes of airway and lung parenchyma in C57BL/6J mice. *J Appl Physiol (1985)* 102: 200–206, 2007. doi:10.1152/japplphysiol.00400.2006.
7. **Brandsma C-A**, **De Vries M**, **Costa R**, **Woldhuis RR**, **Königshoff M**, **Timens W.** Lung ageing and COPD: is there a role for ageing in abnormal tissue repair? *Eur Respir Rev* 26: 170073, 2017. doi:10.1183/16000617.0073-2017.
8. **Frantz C**, **Stewart KM**, **Weaver VM.** The extracellular matrix at a glance. *J Cell Sci* 123: 4195–4200, 2010. doi:10.1242/jcs.023820.
9. **Starcher BC.** Lung elastin and matrix. *Chest* 117: 229s–234s, 2000. doi:10.1378/chest.117.5_suppl_1.229s-a.
10. **De Vries M**, **Faiz A**, **Woldhuis RR**, **Postma DS**, **De Jong TV**, **Sin DD**, **Bossé Y**, **Nickle DC**, **Guryev V**, **Timens W**, **Van Den Berge M**, **Brandsma C-A.** Lung tissue gene-expression signature for the ageing lung in COPD. *Thorax* 73: 609–617, 2018. doi:10.1136/thoraxjnl-2017-210074.
11. **Chow RD**, **Majety M**, **Chen S.** The aging transcriptome and cellular landscape of the human lung in relation to SARS-CoV-2. *Nat Commun* 12: 4, 2021. doi:10.1038/s41467-020-20323-9.
12. **Brandsma C-A**, **Guryev V**, **Timens W**, **Ciconelle A**, **Postma DS**, **Bischoff R**, **Johansson M**, **Ovchinnikova ES**, **Malm J**, **Marko-Varga G**, **Fehniger TE**, **Van Den Berge M**, **Horvatovich P.** Integrated proteogenomic approach identifying a protein signature of COPD and a new splice variant of SORBS1. *Thorax* 75: 180–183, 2020. doi:10.1136/thoraxjnl-2019-213200.
13. **Brandsma C-A**, **Van Den Berge M**, **Postma DS**, **Jonker MR**, **Brouwer S**, **Paré PD**, **Sin DD**, **Bossé Y**, **Laviolette M**, **Karjalainen J**, **Fehrmann RSN**, **Nickle DC**, **Hao K**, **Spanjer AIR**, **Timens W**, **Franke L.** A large lung gene expression study identifying fibulin-5 as a novel player in tissue repair in COPD. *Thorax* 70: 21–32, 2015. doi:10.1136/thoraxjnl-2014-205091.
14. **Hao K**, **Bossé Y**, **Nickle DC**, **Paré PD**, **Postma DS**, **Laviolette M**, **Sandford A**, **Hackett TL**, **Daley D**, **Hogg JC**, **Elliott WM**, **Couture C**, **Lamontagne M**, **Brandsma C-A**, **van den Berge M**, **Koppelman G**, **Reicin AS**, **Nicholson DW**, **Malkov V**, **Derry JM**, **Suver C**, **Tsou JA**, **Kulkarni A**, **Zhang C**, **Vessey R**, **Opiteck GJ**, **Curtis SP**, **Timens W**, **Sin DD.** Lung eQTLs to help reveal the molecular underpinnings of asthma. *PLoS Genet* 8: e1003029, 2012 [Erratum in *PLoS Genet* 8, 2012]. doi:10.1371/journal.pgen.1003029.
15. **Schindelin J**, **Arganda-Carreras I**, **Frise E**, **Kaynig V**, **Longair M**, **Pietzsch T**, **Preibisch S**, **Rueden C**, **Saalfeld S**, **Schmid B**, **Tinevez J-Y**, **White DJ**, **Hartenstein V**, **Eliceiri K**, **Tomancak P**, **Cardona A.** Fiji: an open-source platform for biological-image analysis. *Nat Methods* 9: 676–682, 2012. doi:10.1038/nmeth.2019.
16. **Landini G**, **Martinelli G**, **Piccinini F.** Colour deconvolution: stain unmixing in histological imaging. *Bioinformatics* 37: 1485–1487, 2021. doi:10.1093/bioinformatics/btaa847.
17. **Ruifrok AC**, **Johnston DA.** Quantification of histochemical staining by color deconvolution. *Anal Quant Cytol Histol* 23: 291–299, 2001.
18. **Nguyen D.** Quantifying chromogen intensity in immunohistochemistry via reciprocal intensity. *Protoc Exch* 2: 2013. doi:10.1038/protex.2013.097.
19. **Hunzelmann N**, **Nischt R**, **Brenneisen P**, **Eickert A**, **Krieg T.** Increased deposition of fibulin-2 in solar elastosis and its colocalization with elastic fibres. *Br J Dermatol* 145: 217–222, 2001. doi:10.1046/j.1365-2133.2001.04337.x.
20. **Calhoun C**, **Shivshankar P**, **Saker M**, **Sloane LB**, **Livi CB**, **Sharp ZD**, **Orihuela CJ**, **Adnot S**, **White ES**, **Richardson A**, **Jourdan Le Saux C.** Senescent cells contribute to the physiological remodeling of aged lungs. *J Gerontol A Biol Sci Med Sci* 71: 153–160, 2016. doi:10.1093/gerona/glu241.
21. **Onursal C**, **Dick E**, **Angelidis I**, **Schiller HB**, **Staab-Weijnitz CA.** Collagen biosynthesis, processing, and maturation in lung ageing. *Front Med* 8: 593874, 2021. doi:10.3389/fmed.2021.593874.
22. **Angelidis I**, **Simon LM**, **Fernandez IE**, **Strunz M**, **Mayr CH**, **Greiffo FR**, **Tsitsiridis G**, **Ansari M**, **Graf E**, **Strom T-M**, **Nagendran M**, **Desai T**, **Eickelberg O**, **Mann M**, **Theis FJ**, **Schiller HB.** An atlas of the aging lung mapped by single cell transcriptomics and deep tissue proteomics. *Nat Commun* 10: 963, 2019. doi:10.1038/s41467-019-08831-9.
23. **Cescon M**, **Gattazzo F**, **Chen P**, **Bonaldo P.** Collagen VI at a glance. *J Cell Sci* 128: 3525–3531, 2015. doi:10.1242/jcs.169748.
24. **Mereness JA**, **Bhattacharya S**, **Wang Q**, **Ren Y**, **Pryhuber GS**, **Mariani TJ.** Type VI collagen promotes lung epithelial cell spreading and wound-closure. *PLoS One* 13: e0209095, 2018. doi:10.1371/journal.pone.0209095.
25. **Ansorge HL**, **Meng X**, **Zhang G**, **Veit G**, **Sun M**, **Klement JF**, **Beason DP**, **Soslowsky LJ**, **Koch M**, **Birk DE.** Type XIV collagen regulates

fibrillogenesis. *J Biol Chem* 284: 8427–8438, 2009. doi:10.1074/jbc.M805582200.

26. **Saika S**, **Shiraishi A**, **Saika S**, **Liu C-Y**, **Funderburgh JL**, **Kao CWC**, **Converse RL**, **Kao WWY.** Role of lumican in the corneal epithelium during wound healing. *J Biol Chem* 275: 2607–2612, 2000. doi:10.1074/jbc.275.4.2607.
27. **Yamanaka O**, **Yuan Y**, **Coulson-Thomas VJ**, **Gesteira TF**, **Call MK**, **Zhang Y**, **Zhang J**, **Chang SH**, **Xie C**, **Liu CY**, **Saika S**, **Jester JV**, **Kao WW.** Lumican binds ALK5 to promote epithelium wound healing. *PLoS One* 8: e82730, 2013. doi:10.1371/journal.pone.0082730.
28. **Johnson ER**, **Matthay MA.** Acute lung injury: epidemiology, pathogenesis, and treatment. *J Aerosol Med Pulm Drug Deliv* 23: 243–252, 2010. doi:10.1089/jamp.2009.0775.
29. **Kobayashi N**, **Kostka G**, **Garbe JHO**, **Keene DR**, **Bächinger HP**, **Hanisch F-G**, **Markova D**, **Tsuda T**, **Timpl R**, **Chu M-L**, **Sasaki T.** A comparative analysis of the fibulin protein family. *J Biol Chem* 282: 11805–11816, 2007. doi:10.1074/jbc.M611029200.
30. **Sicot F-X**, **Tsuda T**, **Markova D**, **Klement JF**, **Arita M**, **Zhang R-Z**, **Pan T-C**, **Mecham RP**, **Birk DE**, **Chu M-L.** Fibulin-2 is dispensable for mouse development and elastic fiber formation. *Mol Cell Biol* 28: 1061–1067, 2008. doi:10.1128/MCB.01876-07.
31. **Patel MR**, **Weaver AM.** Astrocyte-derived small extracellular vesicles promote synapse formation via fibulin-2-mediated TGF-β signaling. *Cell Rep* 34: 108829, 2021. doi:10.1016/j.celrep.2021.108829.
32. **Khan SA**, **Dong H**, **Joyce J**, **Sasaki T**, **Chu M-L**, **Tsuda T.** Fibulin-2 is essential for angiotensin II-induced myocardial fibrosis mediated by transforming growth factor (TGF)-β. *Lab Invest* 96: 773–783, 2016. doi:10.1038/labinvest.2016.52.
33. **Tsuda T**, **Wu J**, **Gao E**, **Joyce J**, **Markova D**, **Dong H**, **Liu Y**, **Zhang H**, **Zou Y**, **Gao F**, **Miller T**, **Koch W**, **Ma X**, **Chu M-L.** Loss of fibulin-2 protects against progressive ventricular dysfunction after myocardial infarction. *J Mol Cell Cardiol* 52: 273–282, 2012. doi:10.1016/j.yjmcc.2011.11.001.
34. **Sicard D**, **Haak AJ**, **Choi KM**, **Craig AR**, **Fredenburgh LE**, **Tschumperlin DJ.** Aging and anatomical variations in lung tissue stiffness. *Am J Physiol Lung Cell Mol Physiol* 314: L946–L955, 2018. doi:10.1152/ajplung.00415.2017.
35. **Faarvang A-SA**, **Rørdam Preil SA**, **Nielsen PS**, **Beck HC**, **Kristensen LP**, **Rasmussen LM.** Smoking is associated with lower amounts of arterial type I collagen and decorin. *Atherosclerosis* 247: 201–206, 2016. doi:10.1016/j.atherosclerosis.2016.02.022.
36. **Woenckhaus M**, **Klein-Hitpass L**, **Grepmeier U**, **Merk J**, **Pfeifer M**, **Wild P**, **Bettstetter M**, **Wuensch P**, **Blaszyk H**, **Hartmann A**, **Hofstaedter F**, **Dietmaier W.** Smoking and cancer-related gene expression in bronchial epithelium and non-small-cell lung cancers. *J Pathol* 210: 192–204, 2006. doi:10.1002/path.2039.
37. **Yang S**, **Long M**, **Tachado SD**, **Seng S.** Cigarette smoke modulates PC3 prostate cancer cell migration by altering adhesion molecules and the extracellular matrix. *Mol Med Rep* 12: 6990–6996, 2015. doi:10.3892/mmr.2015.4302.
38. **Lee S**, **Islam MN**, **Boostanpour K**, **Aran D**, **Jin G**, **Christenson S**, **Matthay MA**, **Eckalbar WL**, **Depianto DJ**, **Arron JR**, **Magee L**, **Bhattacharya S**, **Matsumoto R**, **Kubota M**, **Farber DL**, **Bhattacharya J**, **Wolters PJ**, **Bhattacharya M.** Molecular programs of fibrotic change in aging human lung. *Nat Commun* 12: 6309, 2021. doi:10.1038/s41467-021-26603-2.
39. **Wicher SA**, **Roos BB**, **Teske JJ**, **Fang YH**, **Pabelick C**, **Prakash YS.** Aging increases senescence, calcium signaling, and extracellular matrix deposition in human airway smooth muscle. *PLoS One* 16: e0254710, 2021. doi:10.1371/journal.pone.0254710.